ISSN 1070-4272, Russian Journal of Applied Chemistry, 2016, Vol. 89, No. 8, pp. 1265−1273. © Pleiades Publishing, Ltd., 2016.
Original Russian Text © A.I. Abdulagatov, F.F. Orudzhev, M.Kh. Rabadanov, I.M. Abdulagatov, 2016, published in Zhurnal Prikladnoi Khimii, 2016, Vol. 89, No. 8, pp. 1015−1023.

APPLIED ELECTROCHEMISTRY AND METAL CORROSION PROTECTION

Copper Nanowire Arrays Surface Wettability Control Using Atomic Layer Deposition of TiO_2

A. I. Abdulagatov[a,b], F. F. Orudzhev[b], M. Kh. Rabadanov[b], and I. M. Abdulagatov[b]*

[a] *University of Colorado in Boulder, Boulder, CO 80309, U.S.A.*
[b] *Dagestan State University, Makhachkala, ul. Gadzhieva 43a, Dagestan, 367018 Russia*
* *e-mail: ilmutdina@gmail.com*

Received July 4, 2016

Abstract—Template two step electrodeposition method and atomic layer deposition were used to synthesize copper nanowires of varied length (1.2 to 26.2 μm) and copper nanowires coated with titanium dioxide. As a result of the atomic layer deposition of TiO_2, coated nanowires demonstrated an up to 10-fold decrease in the wetting angle, compared with uncoated nanowires. It was found the dissipation rate is substantially higher for nanowires coated by the atomic layer deposition method (100 s) as compared with the uncoated copper nanowires (400 s), which assumes the positive properties of water propagation along the surface, necessary for improving the heat transfer. It was also found that the water contact angle for uncoated nanowires and those coated with TiO_2 by the atomic layer deposition (ALD) gradually increases as the samples are kept in air. A gradual increase in wettability was also observed for smooth silicon wafers coated by ALD of TiO_2, which were exposed to air. On the coated silicon substrates, the wetting angle gradually increased from 10° to approximately 56° in the course of four days. In addition, it was shown that copper nanowires coated with TiO_2 by the atomic layer deposition method have an excellent corrosion resistance, compared with uncoated nanowires, when brought in contact with air and water.

DOI: 10.1134/S1070427216080085

The problems of controlling the surface wettability have been attracting attention in the literature due to the demands in widely differing areas, such as microfluidics [1], cell adhesion [2, 3], moisture condensation [4], and intensification of the heat exchange in heating and cooling systems [5, 6]. A vast number of methods for obtaining surfaces with controlled wettability have been developed. Among those, two categories can be distinguished: chemical (chemical vapor deposition [7], self-assembly [8–10], ion exchange [11] and photodecomposition [12]) and physical, based on the change in the surface roughness (melting of polymers [13], ionic polymerization [14], and laser etching [15]).

The best studied are silicon surfaces or surfaces of some expensive materials, such as gold [10]. In recent years, gained popularity the application of copper as an important construction material to enhance heat transfer, in steam condensers at electric power plants, and heat sinks for cooling of microelectronic using the surface modification of the wettability gradient [16–18]. The problems of thermal control and heat transfer in boiling have been the subject of intense research during the last decades [19, 20]. Some of the studies were concerned with the intensification of the pool boiling due to the decrease in the wetting contant angle (CA) via chemical modification of the surface. In particular, a significant increase in the critical heat flux was reported as a result of experiments in which titanium oxide and silicon oxide coatings were used [20–22]. In these cases, the oxides were used to improve the intermolecular attraction between the solid and liquid phases to improve the efficiency of heat transfer processes.

Typically, oxides are deposited onto planar substrates by gas phase metal-organic chemical vapor deposition (MOCVD), plasma-enhanced chemical vapor deposition (PECVD), magnetron sputtering [22], and solution-

based technique [21, 22]. It was reported that the heat transfer can be improved by making larger the boiling surface area. The increase in the critical heat flux was demonstrated for porous surfaces, tubes, particles and nanowires of copper and silicon [24, 25].

Copper nanowires are particularly attractive as substrates because of the ease of fabrication, high heat conductivity, and large surface area. However, the issues associated with controlling the wettability of the nanowire arrays have been poorly studied because surfaces with highly developed structure pose a severe problem for the conventional coating methods (MOCVD, PECVD, etc.). The atomic layer deposition (ALD) is a method for obtaining thin films, which has a unique capability of producing rather conformal films on highly developed surfaces [26]. The ALD method was first developed under the name of "molecular layering" in the early 1960's in the USSR under the supervision of V.B. Aleskovskii and was later developed by his students [27]. The conformal deposition on textured surfaces with aspect ratio as large as 5000 : 1 was previously demonstrated with ZnO ALD and pore size of 19 nm [28]. Thus, the ALD provides us with unprecedented opportunity of a conformal coating of the high surface area copper nanowires with a superhydrophilic oxide to improve it's wettability. In addition, to advantages of the ALD can be attributed the corrosion protection of copper nanowires working under severe physical conditions, such as water boiling. The oxidation and dissolution of copper can restrict the heat-transfer efficiency, which is known to be a problem in heat exchangers [29].

Our goal in the present study was to manufacture high surface area copper by texturing it as well as improving its wettability by chemical surface modification. Titanium dioxide was material of choice for coating the nanowires owing to its hydrophilic properties and stability in water [30]. We examined specific features of the wettability of copper nanowires of various length with and without TiO_2 coating.

EXPERIMENTAL

Arrays of Cu nanowires were fabricated by two-step electrodeposition process. A template of porous anodic aluminum oxide (AAO) with pore size of about 250 nm (Whatman 6809–5502) was used to grow an array of Cu nanowires. The electrolyte solution was composed of 60 g L^{-1} of copper pyrophosphate ($Cu_2P_2O_7 \cdot H_2O$, Sigma-Aldrich 34469-9), 250 g L^{-1} of potassium pyrophosphate ($K_4P_2O_7$, Sigma-Aldrich 322431-500G), and 20 g L^{-1} of ammonium citrate ($C_6H_{17}O_7$, Fluka 09831). A silicon wafer with a copper coating served as a planar substrate. In the typical fabrication process, a sandwich structure was constructed by stacking a substrate, AAO template, filter paper saturated with an electrolyte solution, and Cu foils, as described in [31]. A dc voltage of –0.8 V was applied between the opposite electrode (Cu) and the substrate plane for 10 min. After that the substrate was released from the sandwiched structure. For the second electrodeposition stage, the substrate with an AAO template on top was placed in a three-electrode galvanic cell. A dc voltage of –1 V relative to the reference electrode (Ag/AgCl) was applied. To obtain an array of Cu nanowires of different length, the electrolysis duration was varied. The arrays of Cu nanowires were then freed from the AAO template by submerging the samples in 2 M NaOH for 2 h, several times washed with distilled water, and dried in a vacuum chamber.

Scanning electron microscopy (SEM) (Jeol Limited JSM-6480LV, Japan) was used to obtain information about the length of nanowires and surface morphology.

Thin AAO films were deposited a viscous flow hot walled type reactor. To deposit a 120 Å thick TiO_2 film, an ALD Al_2O_3 layer with a thickness of 80 Å was prior deposited as a seed layer. The sequential dose of titanium tetrachloride and water into the reactor used to deposit TiO_2, whereas trimethylaluminum (TMA) and water were used to deposit Al_2O_3 [32]. The deposition was performed at 120°C. At this deposition temperature, titanium oxide and aluminum films are amorphous. The chemistry of ALD TiO_2 is well studied and understood and has been shown to result in high quality film [32, 33].

The X-ray photoelectron spectroscopy (XPS) was performed with a Physical Electronics PGHI 5600 spectrometer and a source of monochromatic AlK_α X-ray radiation with photon energy of 1486.6 eV. XPS scans were obtained at electron energy of 187 eV at a resolution of 0.8 eV.

The liquid contact angle was measured with a 1 μL drop of deionized water placed on the samples by the sessile drop method at room temperature under atmospheric pressure. A high resolution camera monitored the droplets by taking images in specific time increments after the droplet was placed. This allowed us to explore the dynamic behavior of the droplet contact angle; which we tested at different surface conditions. The images were processed with First Ten Angstroms visualization

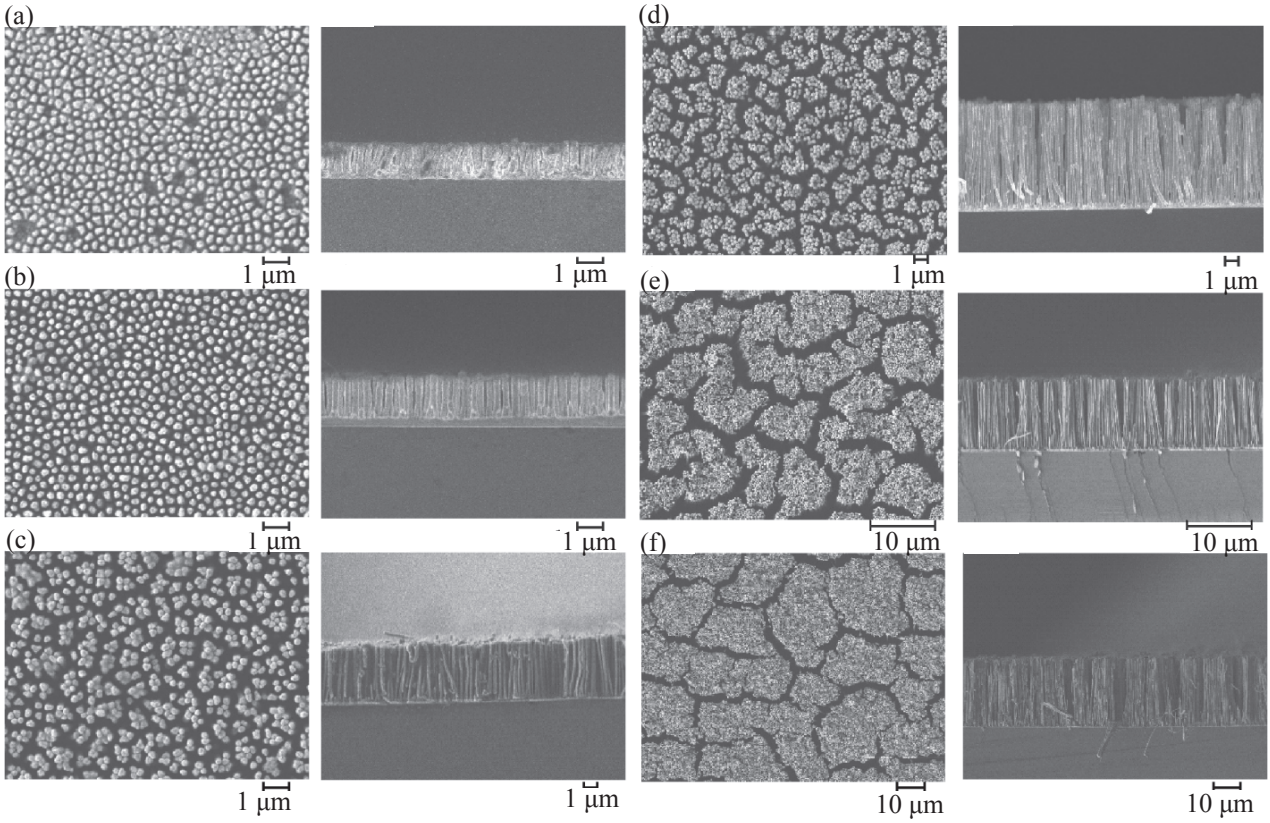

Fig. 1. SEM images of Cu nanowires. (a) 8 min, 1.2 μm; (b) 15 min, 1.6 μm; (c) 30 min, 4.7 μm; (d) 1 h, 8.6 μm; (e) 2 h, 13.7 μm; (f) 4 h, 26.2 μm.

software (First Ten Angstroms, Inc., United States), to determine the contact angles. Nanowire samples were tested once a day. After the measurements, nanowire samples were kept overnight in a desiccator under vacuum to remove moisture from the surface.

In the course of experiments, we avoided exposure of samples with a TiO_2 ALD coating to UV light, since UV radiation know to be able to change its wettability [34].

RESULTS AND DISCUSSION

To improve the heat transfer efficiency of copper-based materials in devices, it is necessary to raise the surface contact area. For this purpose, we synthesized Cu nanowires. Figure 1 shows SEM images of nanowires obtained in the course of 8, 15, 30 min, 1, 2, and 4 h with lengths of, respectively, 1.2, 1.6, 4.7, 8.6, 13.7, and 26.2 μm. It can be seen that the 1.2- and 1.6-μm-long nanowires are arranged more uniformly relative to each other, whereas 1.6 μm long nanowires are more clustered due to the strong capillary forces between long nanowires. It was found that the size of the hollows being formed depends on synthesis parameters. It can also bee seen that the distance between the 1.2- and 1.60 μm nanowires is approximately 0.16 μm, whereas for nanowires with lengths of 4.7 to 26.2 μm, the gap become larger due to the coalescence and vary from 0.42 to 2.8 μm.

It is known that the wetting mechanism on rough surfaces is mostly explained by two theoretical models developed by Vencel and Cassie–Baxter. The wettability of the samples was evaluated by determining the contact angle for water. Figure 2 shows how the contact angle depends on the length of freshly synthesized clean Cu nanowires and nanowires coated with TiO_2 by the ALD method at a water drop size of 1 μL. Measurements were made during the first 24 h after the synthesis. It can be seen that the value of CA for uncoated nanowires begins with 50° at a length of 1.2 μm, reaches a maximum of 100° at a length of 1.6 μm, and then sharply decreases to approximately 30° beginning with a length of 1.6 μm and more. The sharp increase in the CA from 50 to 100° for the uncoated nanowires can be attributed to a transition from the Vencel state to that by Cassie–Baxter, which account for the change of the wetting mechanism as a

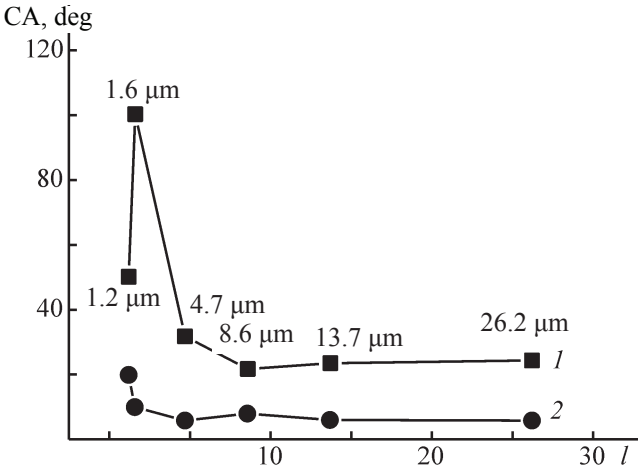

Fig. 2. Dependence of the CA on the length of Cu nanowires (*1*) coated with TiO_2 by the ALD method and (*2*) uncoated.

result of an increase in the nanowire length from 1.2 to 1.6 μm. In this case, a slight increase in the air gap widths between the nanowires at a length of 1.6 μm led to a rise in CA, whereas at a nanowire length of 1.2 μm, the drop height was approximately equal to the length of nanowires. This effect has been theoretically predicted and experimentally observed previously [35, 36]. The effect of nanowire clustering, which begins at a length of 1.6 μm and more for nanowires with lengths of 4.7, 8.6, 13.7, and 26.2 μm, results in that the CA decreases from 100 to approximately 20°. It can be seen that an increase in the nanowire length is accompanied by the effect of clustering and coalescence, which leads to wider air gaps. As a result, the probability of fluid penetration from a drop into the substrate across their contact region becomes higher [37]. This result is in good agreement with the data obtained in [24]. Nevertheless, Bhattacharya et al. [38] reported that the hydrophobicity increases for clustered copper nanowires having a diameter of 200 nm and height of 10 μm when 2 mL water drops are used.

Therefore, the increase in the surface area due to the texturing made the material hydrophobic. The reason why this hydrophobicity is observed is not only the structured state of the surface itself, but also the chemical contamination of the surface of nanowires by reagents used in fabrication and(or) formation of a hydrophobic oxide film due to the oxidation of copper in air. For this nanomaterial to be effectively used in heat-exchange devices, it is necessary to modify its surface to provide hydrophilization without changing its configuration. This is provided by deposition of a TiO_2 film onto the surface of Cu nanowires by the ALD method. The superhydrophilic nature of TiO_2 was first reported by Fujishima's research team [39]. It should be noted that the ALD film with a thickness of only several atomic layers makes possible to screen the surface and create a chemically clean surface due to the substrate shielding effect [40].

The ALD produced TiO_2–Cu nanowires were studied by the XPS method. The XPS spectra obtained after 300 cycles of $TiCl_4$ and H_2O showed the presence of carbon C (51.30 at %) together with Cl (1.42 at %), O (30.25 at %), Ti (11.78 at %), and Cu (5.24 at %). In view of the previously obtained data [41], the ALD growth rate of TiO_2 must be approximately 0.6 Å per cycle, so, the

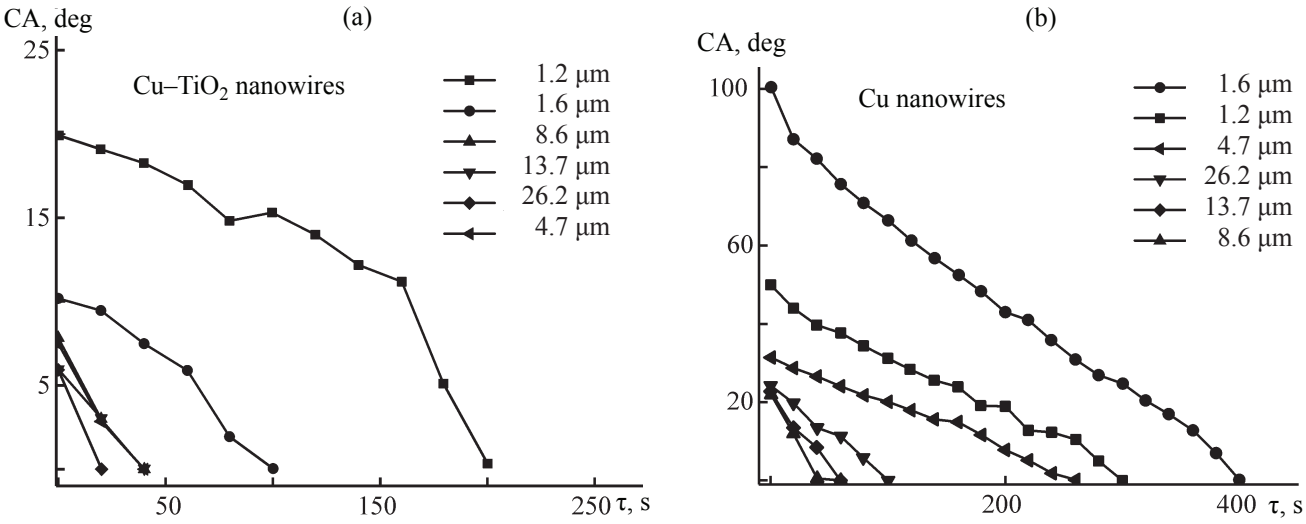

Fig. 3. Variation of the CA for Cu nanowires of various lengths (a) with a 120 Å thick TiO_2 coating formed by the ALD method and (b) without coating. (τ) Time; the same for Figs. 4 and 5.

expected thickness of the TiO_2 film is about 180 Å. The presence of copper in the spectrum indicates, considering the sampling depth of XPS, that a TiO_2 film is not well enough formed on copper substrates. Therefore, an ALD Al_2O_3 film with thickness of 80 Å was pre-deposited as a seed layer prior to deposition of a 120 Å thick TiO_2 film. No traces of copper atoms were observed in the repeated scanning of the samples, and the Cl/Ti atomic percentage ratio was 0.034, which is comparable with the data previously obtained under the same temperature conditions for ALD TiO_2 with a Cl/Ti atomic percentage ratio of 0.047 [42].

The results obtained demonstrated a significant decrease in the CA of water for nanowires coated with TiO_2 by the ALD method, compared with the uncoated nanowires. The nanowires with length of 1.6 μm exhibited the most pronounced decrease in the CA from 100° for uncoated nanowires to 10° for those with a deposited coating. The clustered nanowires having ALD TiO_2 coatings, with lengths of 4.7, 8.6, 13.76, and 26.2 μm, demonstrated the smallest CA values of about 7°. Apparently, the wettability of nanowires prior to their coating with TiO_2 was described by the Cassie–Baxter state because the material was hydrophobic. However, the wettability state can be described by the Vencel model after a TiO_2 film is deposited. The surface of TiO_2 is constituted by highly reactive 5-coordinated Ti atoms, compared with the 6-coordinated Ti in the bulk of TiO_2 [43]. This surface structure accounts for the affinity of TiO_2 toward hydroxyl groups formed as a result of dissociation of chemisorbed water molecules, thereby providing the hydrophilic properties [43].

It can also be seen that the rate of water spreading over the surface was significantly higher for nanowires coated with ALD TiO_2, compared with the uncoated copper nanowires (Figs. 3a and 3b). The water spreading time was 400 s for uncoated nanowires with length of 1.6 μm, whereas for samples with a TiO_2 coating, it was only 100 s. The clustered nanowires show a shorter spreading time, which is presumably accounted for by the strong capillary effects in broad channels. The substantially shorter spreading time for nanowires coated with TiO_2 by the ALD method entails its own positive effect on the water propagation over the surface, which is necessary for improving the heat transfer.

A significant factor in evaluating the efficiency of any functional material is the stability of its characteristics over time. We measured the CA on keeping the samples

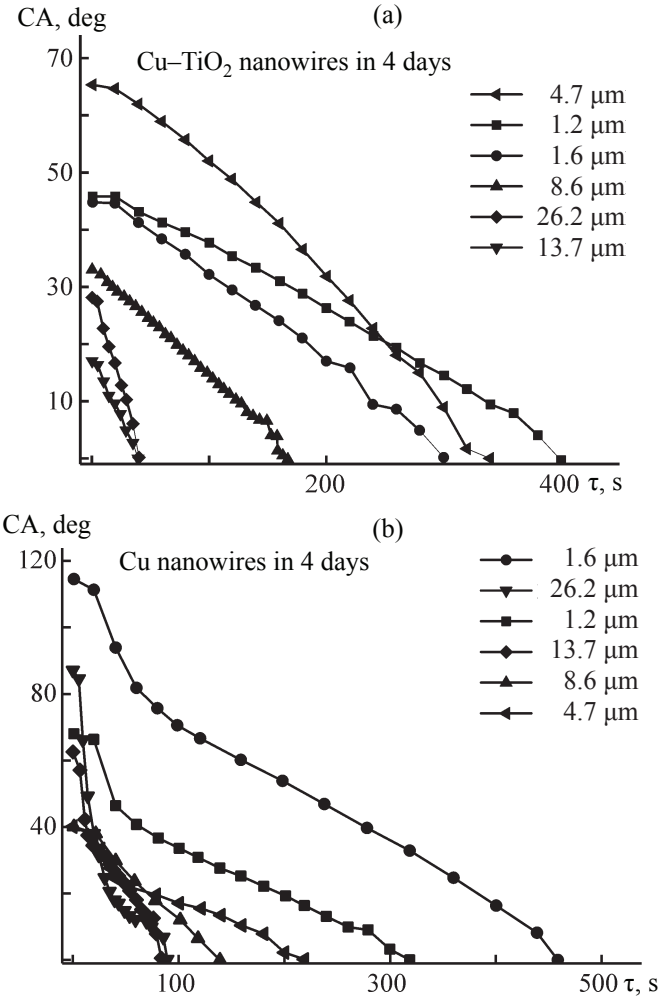

Fig. 4. Variation of the CA for Cu nanowires of various lengths (a) with a 120 Å thick TiO_2 coating formed by the ALD method and (b) without coating on their being kept for four days in air.

in air for a certain time. For example, the results obtained four days after the initial measurements demonstrated an increase in CA for all samples, both with and without a coating. For uncoated nanowires with length of 1.2 μm, a sharp increase in the initial value of CA from 50° to approximately 77° was observed after keeping a sample in air for four days (Fig. 4b). The samples exposed to air also showed a sharp decrease in the CA from 77 to 27° during the first 40 s after a drop is placed, with the subsequent slow dissipation. It can be seen that the exposure to air results in the dissipation rate of a water drop placed on the surface becomes lower. The water dissipation rate, characterized by the slope of the curves in the plots, decreases with increasing initial contact angle. Hence, follows a conclusion that samples exposed to air form stable drops in the upper part of nanowires. This is indicated by the increased stability of droplets

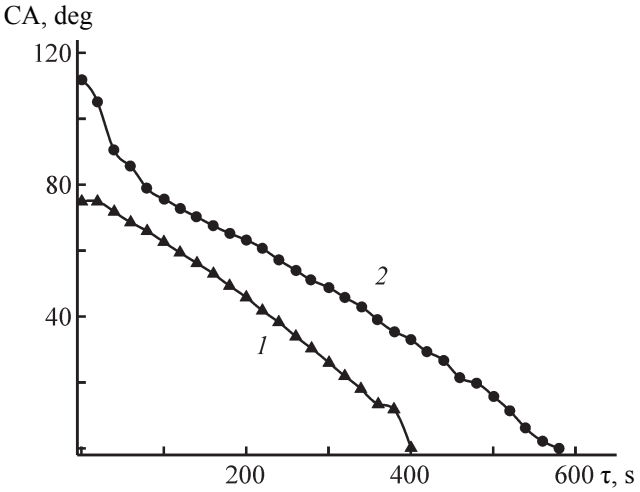

Fig. 5. Variation of the CA for (*2*) Cu nanowires with length of 1.6 μm after 4 days of keeping in air and (*1*) Cu wafer after 30 days keeping in air.

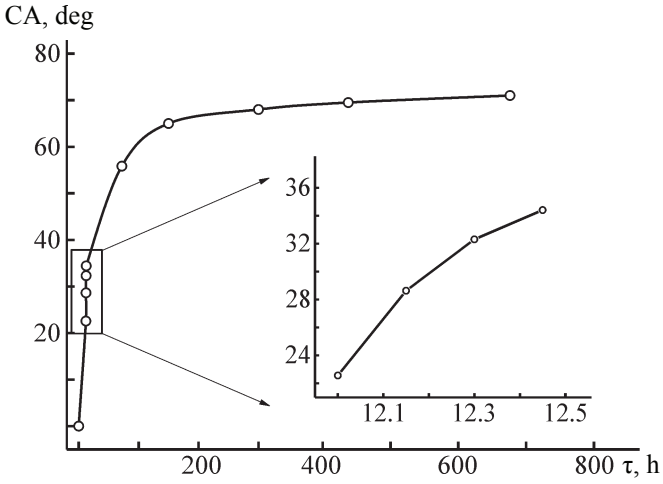

Fig. 6. Variation of the CA for a Si wafer with TiO_2 coating formed by the ALD method after a 720 h exposure to air. (τ) Time, h.

and by their long dissipation time. The decrease in the CA experimentally confirms the transition from the wettability state by Cassie–Baxter to the Vencel state.

It has been suggested in the previous publications that the transition from the Cassie–Baxter state to the Vencel state results from the evaporation of water drops on rough surfaces [44, 45]. However, the change in the wettability state in the given case we attribute to the increase in the CA of the substrates in the course of time. The increase in the initial CA believe to be resulted from a gradual contamination of the surface upon its exposure to air.

The change of the wettability mechanism for nanowires coated with TiO_2 by the ALD method upon their exposure to air (Fig. 4a) shows the same trend as that for uncoated copper nanowires (Fig. 4b). The initial value of the CA and the time at which the full wetting is reached grows with exposure to air. The wettability of the given samples is characterized only by the Vencel state, although a gradual increase in the initial CA is also observed.

It is known that freshly deposited well cleaned oxides have a small CA, which gradually grows after exposure to air [46, 47]. The increase in the CA is attributed to the formation of a layer of organic molecules and statically charged particles on the surface. A similar behavior has been observed previously for metallic surfaces upon adsorption of organic contaminants [48]. The driving factor in the surface modification is decrease in the Gibbs free energy to reach a more thermodynamically stable state [49].

For comparison, we also measured the CA on a flat copper plate and Cu nanowires. Figure 5 shows the difference in the dynamics of CA variation with time for pure Cu nanowires and a smooth copper plate upon their exposure to air. It can be seen that the initial CA for Cu nanowires (112°) exceeds that for the Cu coated wafer (75°). This means that, when the surface is textured, there occurs a transition from the Vencel state to the Cassie-Baxter state. However, the Cassie–Baxter state is metastable for these surfaces because a CA hysteresis characterized by a decrease in CA is observed in the course of time. Because it is known that a wider CA hysteresis is characteristic of the Vencel state [50], it can be said that there occurs a reverse transition from the Cassie–Baxter state to the thermodynamically more favorable Vencel state.

To better understand the change in the wetting behavior of Cu nanowires with a 120 Å thick TiO_2 coating, we also deposited such a film onto a flat silicon wafer under similar conditions and performed CA measurements. Figure 6 shows how the values of the initial CA depend on the duration of exposure to air for the TiO_2–Si sample. For this purpose, coated samples were kept in unsealed containers prior to CA measurements. It can be seen that the CA of a freshly deposited TiO_2–Si sample was about 5° and reached a value of 56° in 96 h (four days). It is seen that this process is fast during the first 75 h after the sample is brought in contact with air. The rate in which the CA measured during the first 12 h after the deposition of TiO_2 increased was 0.3 deg min^{-1}. The wetting angle

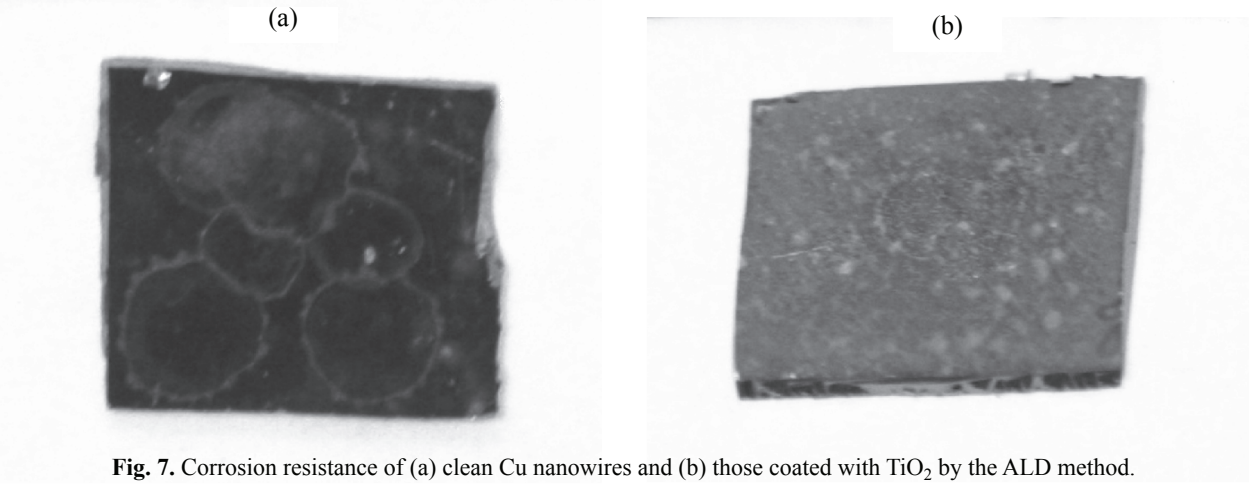

Fig. 7. Corrosion resistance of (a) clean Cu nanowires and (b) those coated with TiO_2 by the ALD method.

measurements made in 720 h (30 days) of exposure of a sample to air demonstrated an insignificant increase in the wetting angle to 71°, which is indicative of the saturation. Consequently, the increase in the initial CA results from the contamination/surface modification of the samples. It is well known that titanium oxide can be easily returned into the hydrophilic state by a UV irradiation [35].

The increase in the CA due to the surface contamination can also be understood on the basis of Fig. 2, in which it can be seen that the 1.2-μm-long nanowires coated with ALD TiO_2 have a larger CA than nanowires with lengths of 4.7 μm and more. If the contamination process is diffusion-controlled and depends on the surface area, shorter nanowires must be faster covered with contaminating substances, compared with the long ones, with the result that the CA of the former will grow faster.

A CA of 80° was reported in [51] for the TiO_2 coating deposited by the ALD method, but the authors disregarded the surface contamination effect. It was shown in another study [46] that the initial CAs vary within the range from 10 to 60° for TiO_2, Al_2O_3, and SiO_2 plates kept in air, depending on the surface contamination level.

The experimental data presented above demonstrate that exposure to air can strongly change the CA. Presumably, the surface energy is modified in the process, therefore, changing the surface wettability of the samples. It can be assumed that the rate at which the wettability changes will depend on the level of pollutants in air in any particular case. It is clear, however, that the nature of an oxide is also an additional factor that plays role in the wettability in various media. In addition, it has been found that the wettability depends not only on the properties of a material, but also on the state of its surface at a given instant of time. A similar effect has been observed for graphene, which exhibited hydrophilic properties immediately after the exfoliation [52].

Supposedly, the oxidation of freshly electroplated copper in air into CuO_x for pure Cu nanowires occurs in parallel with the surface contamination process. The oxidation of copper nanowires is accompanied by a change of the sample coloration in the course of time from bright red to brown. It is also known that that the copper oxidation process is accelerated at high temperatures [53] and in the presence of foreign impurities in water [54]. Microtracks, channels, nanowires, and other copper structures actively used in mictroelectromechanical systems to improve the heat exchange are even more vulnerable against oxidation because of their large surface area. In particular, the formation of agglomerates and topographic changes in the case of copper oxidation may lead to a change in the surface area of nanowires, which impairs the efficiency.

Figure 7 shows images of samples of uncoated nanowires (Fig. 7a) and those coated with ALD TiO_2 (Fig. 7b), taken after 14 days of their exposure to air and water droplets. The color of the freshly synthesized copper nanowires is bright red. The color of the uncoated nanowires changed in 14 days to brown-black, which indicates that copper oxidizes. It can be seen that the corrosion of pure uncoated nanowires was faster at places with water drops. In contrast, the nanowire samples coated with TiO_2 by the ALD method retained their original red color, which points to their good corrosion resistance [55–57].

CONCLUSIONS

It was experimentally demonstrated that coating with TiO_2 by the atomic layer deposition method reduces the

wetting angle of Cu nanowires by up to a factor of 10. When the samples are brought in contact with air, the wetting angles of coated and uncoated samples grow due to changes in the surface properties. For those samples, a gradual transition of the wetting mechanism from that by Vencel to the Cassie–Baxter state was observed. This effect suggests that the wettability of the nanowires is exceedingly sensitive to the chemical state of the surface. In addition, it was shown that a thin film of TiO_2 with an Al_2O_3 seed coating by the atomic layer deposition method provides an excellent protection of copper from oxidation, which is important for preserving the structural features of nanowires in the case of their operation under extreme conditions.

ACKNOWLEDGMENTS

We are grateful to Dr. Wei Wang, former postdoc at the University of Colorado at Boulder, for the assistance in fabrication of copper nanowires and SEM characterization. The study was carried out under Russian Federation State assignments 16.1103.2014/K and 2560.

REFERENCES

1. Zhu, X., Wang, H., Liao, Q., et al., *Exp. Therm. Fluid Sci.,* 2009, vol. 33, no. 6, pp. 947–954.
2. Glassford, S., Chan, K.L.A., Byrne, B., and Kazarian, S.G., *Langmuir*, 2012, vol. 28, no. 6, pp. 3174–3179.
3. Shin, Y.N., Kim, B.S., Ahn, H.H., et al., *Appl. Surf. Sci.*, 2008, vol. 255, no. 2, pp. 293–296.
4. Ju, J., Xiao, K., Yao, X., et al., *Adv. Mater*., 2013, vol. 25, no. 41, pp. 5937–5942.
5. Daniel, S., Chaudhury, M.K., and Chen, J.C., *Science*, 2001, vol. 291, no. 5504, pp. 633–636.
6. Liao, Q., Gu, Y.B., Zhu, X., et al., *J. Enhanced Heat Transfer*, 2007, vol. 14, no. 3, pp. 243–256.
7. Chandesris, B., Soupremanien, U., and Dunoyer, N., *Colloids Surf., A*, 2013, vol. 434, pp. 126–135.
8. Meyyappan, S., Shadnam, M.R., and Amirfazli, A., *Langmuir,* 2008, vol. 24, no. 6, pp. 2892–2899.
9. Yu, X., Wang, Z., Jiang, Y., and Zhang, X., *Langmuir*, 2006, vol. 22, no. 10, pp. 4483–4486.
10. Hu, B., Xue, L., Yang, P., and Han, Y., *Langmuir,* 2010, vol. 26, no. 9, pp. 6350–6356.
11. Wang, L., Peng, B., and Su, Z., *Langmuir,* 2010, vol. 26, no. 14, pp. 12203–12208.
12. Ito, Y., Heydari, M., Hashimoto, A., et al., *Langmuir*, 2007, vol. 23, no. 4, pp. 1845–1850.
13. Zhang, J., Xue, L., and Han, Y., *Langmuir*, 2005, vol. 21, no. 1, pp. 5–8.
14. Li, X., Dai, H., Tan, S., et al., *J. Colloid Interface Sci*., 2009, vol. 340, no. 1, pp. 93–97.
15. Sun, C., Zhao, X.-W., Han, Y.-H., and Gu, Z.-Z., *Thin Solid Films*, 2008, vol. 516, no. 12, pp. 4059–4063.
16. Huang, Z., Lu, Y., Qin, H., et al*., Adv. Eng. Mater*., 2012, vol. 14, no. 7, pp. 491–496.
17. Zhang Yong, C.J., Pi Pihui, Wen Xiufang, et al., *Prog. Chem*., 2011, vol. 23, no. 12, pp. 2457–2465.
18. Hu, Y., Cheng, J., Zhang, W., et al., *Int. J. Heat Mass Transf*., 2013, vol. 67, pp. 416–419.
19. Das, A.K., Das, P.K., and Saha, P., *Exp. Therm. Fluid Sci*., 2007, vol. 31, no. 8, pp. 967–977.
20. Phan, H.T., Caney, N., Marty, P., et al., *Int. J. Heat Mass Transf*., 2009, vol. 52, nos. 23–24, pp. 5459–5471.
21. Wu, W., Bostanci, H., Chow, L.C., et al., *Int. J. Heat Mass Transf*., 2010, vol. 53, nos. 9–10, pp. 1773–1777.
22. Takata, Y., Hidaka, S., Cao, J.M., et al., *Energy*, 2005, vol. 30, nos. 2–4, pp. 209–220.
23. Phan, H.T., Caney, N., Marty, P., et al., *C. R. Méc*., 2009, vol. 337, no. 5, pp. 251–259.
24. Chen, R., Lu, M.-C., Srinivasan, V., et al., *Nano Lett*., 2009, vol. 9, no. 2, pp. 548–553.
25. Patankar, N.A., *Soft Matter*, 2010, vol. 6, no. 8, p. 1613.
26. George, S.M., *Chem. Rev*., 2010, vol. 110, no. 1, pp. 111–131.
27. Malygin, A.A., Drozd, V.E., Malkov, A.A., and Smirnov, V.M., *Chem. Vap. Deposition*, 2015, vol. 21, nos. 10–11–12, pp. 216–240.
28. Elam, J.W., Routkevitch, D., Mardilovich, P.P., and George, S.M., *Chem. Mater*., 2003, vol. 15, no. 18, pp. 3507–3517.
29. Kuźnicka, B., *Eng. Failure Anal*., 2009, vol. 16, no. 7, pp. 2382–2387.
30. Ashkarran, A.A. and Mohammadizadeh, M.R., *Mater. Res. Bull*., 2008, vol. 43, no. 3, pp. 522–530.
31. Taberna, P.L., Mitra, S., Poizot, P., et al., *Nat. Mater*., 2006, vol. 5, no. 7, pp. 567–573.
32. Puurunen, R.L., *J. Appl. Phys*., 2005, vol. 97, no. 12, p. 121301.
33. Ritala, M., Leskelä, M., Nykänen, E., et al., *Thin Solid Films*, 1993, vol. 225, nos. 1–2, pp. 288–295.
34. Caputo, G., Cingolani, R., Cozzoli, P.D., Athanassiou, A., *Phys. Chem. Chem. Phys*., 2009, vol. 11, no. 19, pp. 3692–3700.
35. Kusumaatmaja, H., Blow, M.L., Dupuis, A., and Yeomans, J.M., *EPL (Europhys. Lett.),* 2008, vol. 81, no. 3, p. 36003.

36. Plawsky, J.L., Ojha, M., Chatterjee, A., and Wayner, P.C. Jr., *Chem. Eng. Commun*., 2008, vol. 196, no. 5, pp. 658–696.
37. Gallyamov, M., Nikitin, L., Nikolaev, A., et al., *Kolloid. Zh*., 2007, vol. 69, no. 4, pp. 448–462.
38. Bhattacharya, P., Gohil, S., Mazher, J., *Nanotechnology*, 2008, vol. 19, no. 7, p. 075709.
39. Wang, R., Hashimoto, K., and Fujishima, A., *Nature*, 1997, vol. 388, no. 6641, pp. 431–432.
40. Malygin, A.A., *Soros. Obrazovat. Zh*., 2004, vol. 8, no. 4, pp. 32–37.
41. Aarik, J., Aidla, A., Mändar, H., and Sammelselg, V., *J. Cryst. Growth,* 2000, vol. 220, no. 4, pp. 531–537.
42. Abdulagatov, A.I., Yan, Y., Cooper, J.R., et al., *ACS Appl. Mater. Interfaces*, 2011, vol. 3, no. 12, pp. 593–601.
43. Wang, R., Hashimoto, K., Fujishima, A., et al., *Adv. Mater*., 1998, vol. 10, no. 2, pp. 135–138.
44. McHale, G., Aqil, S., Shirtcliffe, N.J., et al., *Langmuir*, 2005, vol. 21, no. 24, pp. 11053–11060.
45. Tsai, P., Lammertink, R.G.H., Wessling, M., and Lohse, D., *Phys. Rev. Lett*., 2010, vol. 104, no. 11, pp. 116102.
46. Watanabe, T., *J. Ceram. Soc. Japan*, 2009, vol. 117, no. 1372, pp. 1285–1292.
47. Kietzig, A.-M., Hatzikiriakos, S.G., and Englezos, P., *Langmuir*, 2009, vol. 25, no. 8, pp. 4821–4827.
48. Birch, W., Carré, A., and Mittal, K.L., *Developments in Surface Contamination and Cleaning*, New York: Elsevier, 2008.
49. Kung, H.H., *Transition Metal Oxides–-Surface Chemistry and Catalysis*, Amsterdam Elsevier, 1989, vol. 45.
50. McHale, G., Shirtcliffe, N.J., and Newton, M.I., *Langmuir*, 2004, vol. 20, no. 23, pp. 10146–10149.
51. Triani, G., Campbell, J.A., and Evans, P.J., *Thin Solid Films*, 2010, vol. 518, no. 12, pp. 3182–3189.
52. Li, Z., Wang, Y., Kozbial, A., et al., *Nat. Mater*., 2013, vol. 12, no. 10, pp. 925–931.
53. Zheng, J., Bogaerts, W., and Lorenzetto, P., *Fusion Eng. Des*., 2002, vols. 61–62, pp. 649–657.
54. Sobue, K., Sugahara, A., Nakata, T., et al., *Surf. Coat. Technol*., 2003, vols. 169–170, pp. 662–665.
55. Shan, C.X., Hou, X., and Choy, K.-L., *Surf. Coat. Technol*., 2008, vol. 202, no. 11, pp. 2399–2402.
56. Shan, C.X., Hou, X., Choy, K.-L., and Choquet, P., *Surf. Coat. Technol*., 2008, vol. 202, no. 10, pp. 2147–2151.
57. Abdulagatov, A., Yan, Y., Cooper, J.R., et al., *ACS Appl. Mater. Interfaces*, 2011, vol. 3, pp. 4593–4601.